

ITIC Derivative Acceptors for Ternary Organic Solar Cells: Fine-Tuning of Absorption Bands, LUMO Energy Levels, and Cascade Charge Transfer

*Seungyun Baik,^{1,†} Dong Won Kim,^{2,†} Hyun-Sik Kang,¹ Seung Hwa Hong,² Sungjin Park,²
Byeong-Kwan An,^{1,*} Soo Young Park^{2,*}*

¹Department of Chemistry, The Catholic University of Korea, 43 Jibong-ro, Wonmi-gu, Bucheon, Gyeonggi-do, 14662, Korea.

²Lab of Supramolecular Optoelectronic Materials, Department of Materials Science and Engineering, Seoul National University, 1 Gwanak-ro, Gwanak-gu, Seoul, 151-744, Korea

*Corresponding authors. E-mail: bk.an@catholic.ac.kr, parsky@snu.ac.kr

†These authors contributed equally to this work.

CONTENTS

1. Materials and General Methods	2
2. Synthesis	2
3. Electrochemical Properties of IND Derivatives	8
4. Thermal Properties of ITIC Derivatives	9
5. Optical Properties and Energy Levels of ITIC Derivatives in Film	10
6. Orbital Diagrams of ITIC Derivatives Calculated by DFT calculations	11
7. PBDB-T:Acceptors-based Binary Solar Cells	12
8. DFT-Optimized Structures of ITIC, ITBTD and ITICS	12
9. PBDB-T:ITIC:A₂ Acceptor-based Ternary Solar Cells	13

1. Materials and General Methods

IND and ITIC derivatives were prepared by the method described below. Their chemical structures were fully confirmed by $^1\text{H-NMR}$, $^{19}\text{F-NMR}$, FT-IR, Mass spectroscopy, and elemental analysis. $^1\text{H-NMR}$ and $^{19}\text{F-NMR}$ spectra were recorded on a Bruker Ascend 500 spectrometer and Avance III HD respectively. IR spectra were recorded on a Bruker TENSOR II (ATR). Mass spectra were acquired through the JEOL JMS-700 instrument. Elemental analyses were performed on Flash2000 (Thermo Fisher Scientific, Germany). UV-vis absorption spectra were recorded on a Shimadzu UV-3100 UV-VIS-NIR spectrometer. The DSC and TGA measurements were recorded using DSC 4000 (Perkin Elmer) and TGA 4000 (Perkin Elmer), respectively. Cyclic voltammetry data were measured on an AUTOLAB/PG-STAT12 model system by using Bu_4NPF_6 (0.1 M) in dichloromethane as electrolyte at a scan rate of 50 mV/s. Potentials were referenced to the ferrocenium/ferrocene couple by using ferrocene as an internal standard. The photoemission spectroscopy was measured using a Hitachi High Tech (AC-2). AFM measurement (tapping mode) was performed on a NX-10 (Park Systems). Density functional theory (DFT) calculations were carried out in the gas phase using Gaussian 09 quantum-chemical package. The geometry optimizations were performed using B3LYP functionals and 6-31G+(d,p) basis set.

SCLC measurement.

For space-charge-limited currents (SCLC) measurement, hole-only and electron-only devices were fabricated respectively with the configuration of ITO/PEDOT:PSS/BHJ layer/ MoO_3 (10 nm)/Ag (100 nm) and ITO/ ZnO /BHJ layer/PFN-Br/Al. The SCLC mobility was determined by using dark current under forward bias. The SCLC mobilities were calculated using the below equation:

$$J = \frac{9}{8} \varepsilon_r \varepsilon_0 \mu_0 \frac{V^2}{L^3}$$

where J is the current density, ε_r is the dielectric constant of the organic material (dielectric constant assumed to be 3), ε_0 is the permittivity of free space, μ_0 is the zero-field hole mobility, L is the polymer thickness, and the effective voltage, $V = V_{\text{appl}} - V_{\text{bi}}$, where V_{appl} is the applied voltage to the device, and V_{bi} is the built-in voltage. The SCLC mobility was calculated from the slope ($J \sim V^2$).

Photovoltaic Device Fabrication and Evaluation.

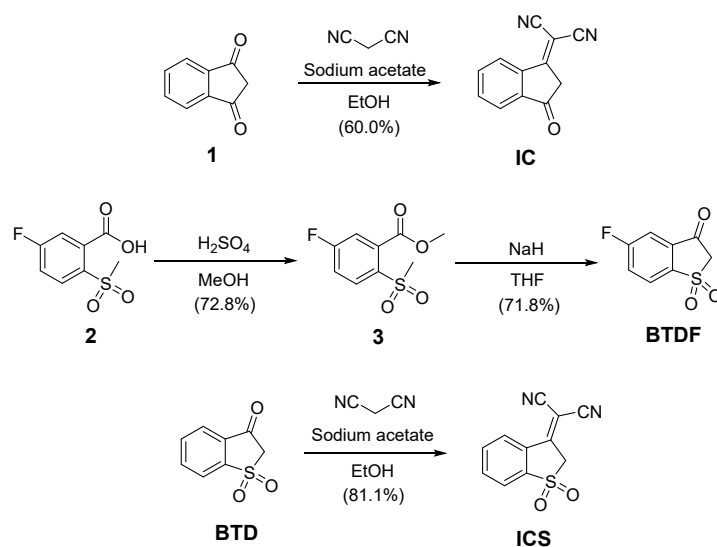
Indium tin oxide glass substrate with a sheet resistance of $15 \Omega \text{ sq}^{-1}$ were purchased from AMG tech (Korea). PBDB-T and PFN were purchased from Solarmer Materials Inc and 1-Materials, respectively. The patterned indium tin oxide (ITO) glass substrates ($1.5 \times 1.5 \text{ cm}^2$) were ultrasonicated for 20 min in the order of DI water, acetone, and isopropanol after cleaning with a detergent. Before spin coating, all of the glass/ITO substrates were treated using UV-ozone equipment for 10 min. To form the hole transport layer, a PEDOT:PSS (Clavious P VP

AI 4083) was spin-coated at 5000 rpm for 30 s on ITO substrate, and then dried on a hot plate at 160 °C for 10 min in an ambient condition. For the deposition of photoactive layers, all of the substrate were moved to a glove box filled with nitrogen gas. For binary solution, PBDB-T and acceptor (1:1 w/w ratio) in chlorobenzene: 1,8 DIO (99.5:0.5 v/v ratio) were fully dissolved at 50 °C for over 3 hours before use. For optimum ternary blend solutions, PBDB-T, ITIC, and acceptor 2 (1:0.95:0.05 w/w ratio) were fully dissolved at 50 °C for over 3 hours before use. The total solution concentration of all blend solutions is 22 mg/mL. The blend solution was spin-coated at 2200 rpm and dried at 120–130 °C for 10 min. PFN (5 nm) was spin-coated on photoactive layer. Finally, a 100 nm layer of Al was deposited by thermal evaporation under a vacuum of 10⁻⁶ Torr. The current density (*J*)–voltage (*V*) characteristics of the solar cells were measured by using a Keithley 4200 source measurement unit. The solar cell performances were characterized under AM 1.5G condition with an illumination intensity of 100 mW cm⁻², as generated using an Oriel Sol3A solar simulator (Oriel model 9023A). The measurements were performed using a mask with aperture area of 0.04 cm² under an ambient atmosphere.

2. Synthesis

The compound **1** was purchased from Alfa Aesar, and the compound **2** and Benzo[*b*]thiophen-3(2*H*)-one 1,1-dioxide (**BTD**) were purchased from Fluorochem. IDTT-CHO was purchased from Solarmer Materials Inc. All other chemicals were used as received.

2-1. Synthesis of Terminal IND Derivatives



Scheme S1. Synthetic routes of terminal IND derivatives.

2-(3-Oxo-2,3-dihydro-1*H*-inden-1-ylidene)malononitrile (IC). Indane-1,3-dione (**1**) (1.33 g, 9.08 mmol) and malononitrile (1.20 g, 18.17 mmol) were dissolved in 50 ml absolute ethanol, and then anhydrous sodium acetate

(0.98 g, 11.81 mmol) was added. After 40 min stirring at room temperature, the mixture was poured into water, and acidified to pH 1 by slowly adding a 2N solution of HCl in water. The precipitate was filtered and recrystallized from acetic acid to give the product as a brown solid (1.06 g, 60.0 %). ¹H NMR (500 MHz; CDCl₃) δ 8.66 (d, *J* = 7.5 Hz, 1H), 7.99 (d, *J* = 7.0 Hz, 1H), 7.92–7.84 (m, 2H), 3.74 (s, 2H).

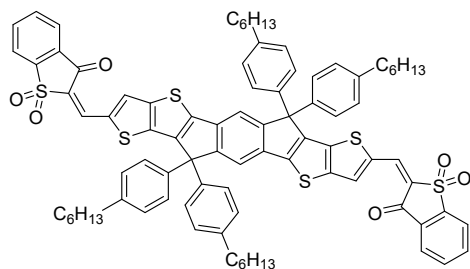
Methyl-5-fluoro-2-(methylsulfonyl)benzoate (3). A suspension of 5-fluoro-2-(methylsulphonyl)benzoic acid (**2**) (200 mg, 0.917 mmol) in MeOH (10 mL) was treated with conc. sulphuric acid (73 μL) in 50 mL Schlenk flask and the resulting mixture was heated at 80 °C for 18 h. The mixture was concentrated under reduced pressure. The residue was dissolved in EtOAc then washed with water, dried on MgSO₄, filtered and concentrated. The residue was purified by silica gel column chromatography by using a dichloromethane as the eluent to yield the product as a solid (155 mg, 72.8%). ¹H NMR (500 MHz; CDCl₃) δ 8.15 (dd, *J* = 10.0, 5.0 Hz, 1H), 7.41 (dd, *J* = 10.0, 5.0 Hz, *J* = 8.5, 1H), 7.35–7.32 (m, 1H), 3.99 (s, 3H), 3.35 (s, 3H).

5-Fluorobenzo[*b*]thiophen-3(2*H*)-one 1,1-dioxide (BTDF). A solution of **3** (600 mg, 2.58 mmol) in anhydrous THF (45 ml) was treated with NaH (60% dispersion in mineral oil) (120 mg, 3.00 mmol) and stirred at room temperature for overnight. The reaction was quenched with water. And then AcOEt and a 2N solution of HCl in water were added and the organic phase was washed with brine, dried on MgSO₄, filtered and concentrated. The residue was purified by silica gel column chromatography by using a dichloromethane as the eluent to yield the product as a white solid (371 mg, 71.8%). ¹H NMR (500 MHz; CDCl₃) δ 8.04–8.01 (m, 1H), 7.66–7.63 (m, 2H), 4.16 (s, 2H). ¹⁹F NMR (282.37 MHz, CDCl₃) δ = -102.96 (s, 1F).

2-(1,1-Dioxidobenzo[*b*]thiophen-3(2*H*)-ylidene)malononitrile (ICS). Benzo[*b*]thiophen-3(2*H*)-one 1,1-dioxide (**BTD**) (1.00 g, 5.49 mmol) and malononitrile (0.54 g, 8.23 mmol) were dissolved in absolute ethanol (50 mL), and then sodium acetate (0.45 g, 5.49 mmol) was added and stirred for 1 h at 80 °C. The pH of the solution was adjusted to pH 1 by slowly adding a 2N solution of HCl in water. The resulting suspension was filtered and washed with water, and dried to afford the product as a white solid (1.02 g, 80.7%). ¹H NMR (500 MHz; CDCl₃) δ 8.69 (d, *J* = 15.0 Hz, 1H), 8.01–7.87 (m, 3H), 4.56 (s, 2H).

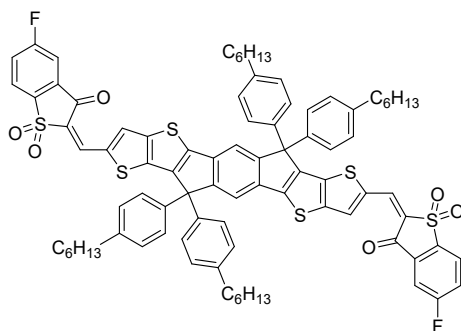
2-2. Synthesis of Symmetric ITIC Derivatives

ITBTD. To a 100 mL round bottom flask were added IDTT-CHO (100 mg, 0.093 mmol), BTD (42.4 mg, 0.232 mmol) and acetic acid (10 mL). Thereafter, piperidine (2 μL) was added. The mixture was stirred at 110 °C for 16 h. After cooling to room temperature, the mixture was poured into water (100 mL), filtered, and washed with water. The residue was purified by column chromatography on silica gel using ethyl acetate/*n*-hexane (1:10) as the eluent, and recrystallized using dichloromethane and *n*-hexane to yield the product as a dark red solid (66 mg, 50.5%). ¹H NMR (500 MHz; CDCl₃) δ 8.52 (s, 2H), 8.10 (d, *J* = 10.0 Hz, 2H), 8.06 (d, *J* = 10.0 Hz, 2H), 7.96 (s, 2H), 7.92 (t, 2H), 7.83 (t, 2H), 7.65 (s, 2H), 7.21–7.14 (m, 16H), 2.57 (t, 8H), 1.62–1.58 (m, 8H), 1.35–1.26 (m, 24H), 0.88–0.85 (m, 12H). FT-IR (cm⁻¹): 1694 (C=O), 1295 (O=S=O). Mass (FAB, *m/z*): calcd for C₈₆H₈₂O₆S₆: 1403.96, found: 1403 (M⁺). Anal. Calcd for C₈₆H₈₂O₆S₆: C, 73.57; H, 5.89. Found: C, 73.42; H, 5.77%.



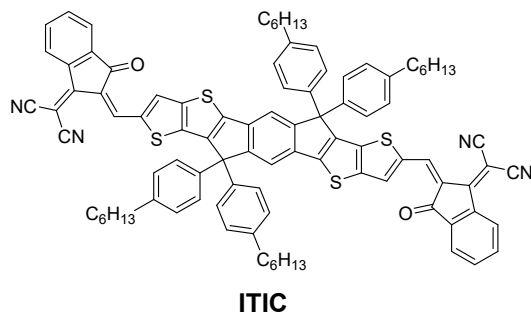
ITBTD

ITBTDF. To a 100 mL round bottom flask were added IDTT-CHO (200 mg, 0.186 mmol), BTDF (149 mg, 0.743 mmol) and acetic acid (20 mL). Thereafter, piperidine (4 μ L) was added. The mixture was stirred at 120 $^{\circ}$ C for 36 h. After cooling to room temperature, the mixture was poured into water (100 mL), filtered, and washed with water. The residue was purified by column chromatography on silica gel using ethyl acetate/*n*-hexane (1:10) as the eluent, and recrystallized using dichloromethane and *n*-hexane to yield the product as a dark brown solid (130 mg, 48.5%). ^1H NMR (500 MHz; CDCl_3) δ 8.52 (s, 2H), 8.10 (d, $J = 10.0$ Hz, 2H), 8.06 (dd, $J = 8.5, 4.5$ Hz, 2H), 7.96 (s, 2H), 7.72 (d, $J = 7.5$, 2H), 7.65 (s, 2H), 7.58 (t, 2H), 7.21–7.12 (m, 16H), 2.57 (t, 8H), 1.62–1.58 (m, 8H), 1.36–1.25 (m, 24H), 0.87–0.85 (m, 12H). ^{19}F NMR (282.37 MHz, CDCl_3) $\delta = -103.00$ (s, 1F). FT-IR (cm^{-1}): 1687 (C=O), 1262 (O=S=O). Mass (FAB, m/z): calcd for $\text{C}_{86}\text{H}_{88}\text{F}_2\text{O}_6\text{S}_6$: 1439.94, found: 1439 (M^+). Anal. Calcd for $\text{C}_{86}\text{H}_{82}\text{O}_6\text{S}_6$: C, 71.74; H, 5.60. Found: C, 71.88; H, 5.57%.

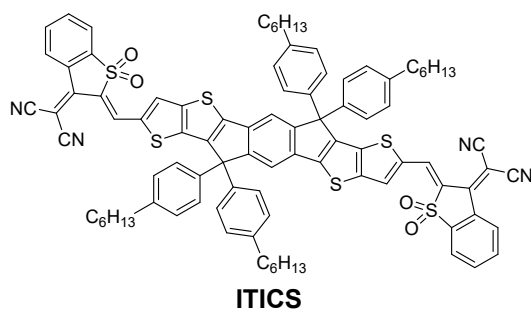


ITBTDF

ITIC. To a 100 mL round bottom flask were added IDTT-CHO (200 mg, 0.186 mmol), IC (180 mg, 0.930 mmol) and chloroform (45 mL). Thereafter, pyridine (1.6 mL) was added. The mixture was stirred at room temperature for 10 h. The reaction mixture was poured into methanol (150 mL), filtered, and washed with methanol. The residue was purified by column chromatography on silica gel using dichloromethane/*n*-hexane (1:1) as the eluent to yield the product as a dark brown solid (230 mg, 85.8%). ^1H NMR (500 MHz; CDCl_3) δ 8.86 (s, 2H), 8.68 (d, $J = 7.5$ Hz, 2H), 8.22 (s, 2H), 7.91 (d, $J = 6.5$ Hz, 2H), 7.78–7.71 (m, 4H), 7.63 (s, 2H), 7.22 (d, $J = 8.5$ Hz, 8H), 7.14 (d, $J = 8.5$ Hz, 8H), 2.57 (t, 8H), 1.59 (pentet, 8H), 1.35–1.26 (m, 24H), 0.87–0.84 (t, 12H). FT-IR (cm^{-1}): 2218 (–CN), 1698 (C=O). Mass (FAB, m/z): calcd for $\text{C}_{94}\text{H}_{82}\text{N}_4\text{O}_2\text{S}_4$: 1427.96, found: 1427 (M^+).



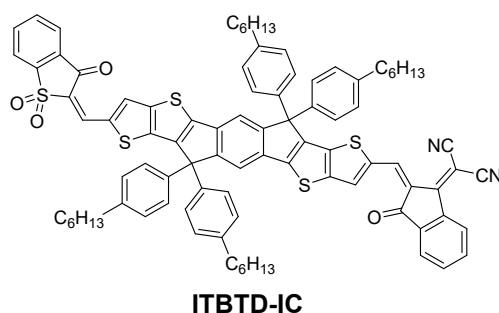
ITICS. To a 100 mL round bottom flask were added IDTT-CHO (300 mg, 0.279 mmol), ICS (160 mg, 0.697 mmol) and acetic anhydride (60 mL). The mixture was stirred at 120 °C for 5 h. After cooling to room temperature, the mixture was poured into water (300 mL), filtered, and washed with water. The crude was recrystallized using dichloromethane and methanol to obtain the product as a dark brown solid (341 mg, 81.5%). ¹H NMR (500 MHz; CDCl₃) δ 8.85 (d, *J* = 7.5 Hz, 2H), 8.57 (s, 2H), 8.56 (s, 2H), 8.00 (d, *J* = 7.0 Hz, 2H), 7.89–7.83 (m, 4H), 7.67 (s, 2H), 7.16–7.13 (m, 16H), 2.58 (t, 8H), 1.63–1.58 (m, 8H), 1.35–1.25 (m, 24H), 0.88–0.84 (m, 12H). FT-IR (cm⁻¹): 2218 (–CN), 1290 (O=S=O). Mass (FAB, *m/z*): calcd for C₉₄H₈₂N₄O₄S₆: 1500.05 found: 1499 (M⁺).



2-3. Synthesis of Asymmetric ITIC Derivatives

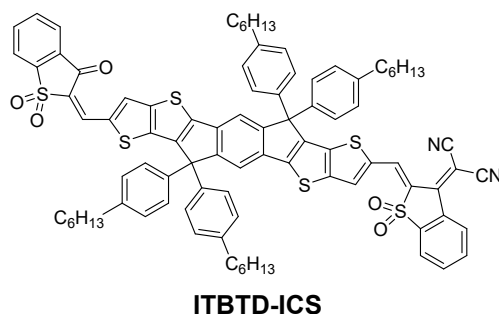
ITBTD-IC. To a 100 mL round bottom flask were added IDTT-CHO (400 mg, 0.372 mmol), BTD (67.8 mg, 0.372 mmol) and acetic acid (40 mL). Thereafter, piperidine (2 μL) was added. The mixture was stirred at 110 °C for 16 h. After cooling to room temperature, the mixture was poured into water (100 mL), filtered, and washed with water. The residue was isolated by column chromatography on silica gel using ethyl acetate/*n*-hexane (1:10) as the eluent to give the intermediate compound with the *R_f* value of 0.2~0.3 (ethyl acetate:*n*-hexane (1:5)) on a TLC. The intermediate compound was used without further purification for next step reaction. To a 25 mL round bottom flask were added the intermediate compound (52 mg, 0.042 mmol), IC (20.4 mg, 0.104 mmol) and chloroform (10 mL). Thereafter, pyridine (0.4 mL) was added. The mixture was stirred at room temperature for 9 h. The reaction mixture was poured into methanol (80 mL), filtered, and washed with methanol. The residue was purified by column chromatography on silica gel using dichloromethane/*n*-hexane (1:2) as the eluent to yield the product as a dark brown solid (15.6 mg, 26.2%). ¹H NMR (500 MHz; CDCl₃) δ 8.87 (s, 1H), 8.68 (d, *J* = 7.5 Hz, 1H), 8.52 (s, 1H), 8.21 (s, 1H), 8.10 (d, *J* = 7.5 Hz, 1H), 8.06 (d, *J* = 7.5 Hz, 1H), 7.96 (s, 1H), 7.93–7.91 (m, 2H), 7.84 (t, 1H), 7.77–7.74 (m, 2H), 7.64 (d, *J* = 7.5 Hz, 2H), 7.22 (d, *J* = 8.5 Hz, 4H), 7.17–7.12 (m, 12H), 2.57 (t, 8H), 1.60–1.58 (m, 8H), 1.33–1.25 (m, 24H), 0.87–0.84 (m, 12H). FT-IR (cm⁻¹): 2217 (–CN), 1700 (C=O), 1282

(O=S=O). Mass (FAB, m/z): calcd for $C_{90}H_{82}N_2O_4S_5$: 1415.96, found: 1415(M^+). Anal. Calcd for $C_{90}H_{82}N_2O_4S_5$: C, 76.34; H, 5.84; N, 1.98. Found: C, 76.38; H, 5.74; N, 2.04%.



ITBTD-IC

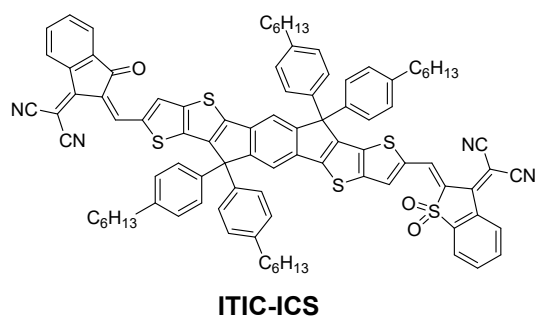
ITBTD-ICS. The reaction procedure was performed in the same way as ITBTD-IC until the preparation of the intermediate compound. To a 100 mL round bottom flask were added the intermediate compound (120 mg, 0.097 mmol), ICS (30 mg, 0.117 mmol) and acetic anhydride (15 mL). The mixture was stirred at 120 °C for 5 h. After cooling to room temperature, the mixture was poured into water (100 mL), filtered, and washed with water. The residue was purified by column chromatography on silica gel using dichloromethane/*n*-hexane (1:2) as the eluent to yield the product as a dark brown solid (63 mg, 44.8%). ¹H NMR (500 MHz; CDCl₃) δ 8.85 (d, *J* = 7.5 Hz, 1H), 8.57 (d, *J* = 2.5 Hz, 2H), 8.52 (s, 1H), 8.10 (d, *J* = 7.5 Hz, 1H), 8.06 (d, *J* = 7.5 Hz, 1H), 8.01 (d, *J* = 7.5 Hz, 1H), 7.96 (s, 1H), 7.92–7.82 (m, 4H), 7.66 (d, *J* = 7.0 Hz, 2H), 7.17–7.12 (m, 16H), 2.57 (t, 8H), 1.61–1.58 (m, 8H), 1.34–1.28 (m, 24H), 0.87–0.83 (m, 12H). FT-IR (cm⁻¹): 2214 (–CN), 1697 (C=O), 1284 (O=S=O). Mass (FAB, m/z): calcd for $C_{89}H_{82}N_2O_5S_6$: 1452.00 found: 1451 (M^+). Anal. Calcd for $C_{89}H_{82}N_2O_5S_6$: C, 73.62; H, 5.69; N, 1.93. Found: C, 73.23; H, 5.52; N, 2.00%.



ITBTD-ICS

ITIC-ICS. To a 100 mL round bottom flask were added IDTT-CHO (200 mg, 0.186 mmol), IC (36 mg, 0.186 mmol) and chloroform (40 mL). Thereafter, pyridine (1.0 mL) was added. The mixture was stirred at room temperature for 10 h. The reaction mixture was poured into methanol (200 mL), filtered, and washed with methanol. The crude intermediate was used without further purification. To a 100 mL round bottom flask were added the intermediate compound (100 mg), ICS (100 mg, 0.434 mmol) and acetic anhydride (40 mL). The mixture was stirred at 120 °C for 3 h. After cooling to room temperature, the mixture was poured into water (300 mL), filtered, and washed with water. The residue was purified by column chromatography on silica gel using ethyl acetate/*n*-hexane (1:10) as the eluent to yield the product as a dark brown solid (66 mg, 14.0%). ¹H NMR

(500 MHz; CDCl₃) δ 8.87 (s, 1H), 8.85 (d, $J = 7.5$ Hz, 1H), 8.68 (d, $J = 7.5$ Hz, 1H) 8.57 (d, $J = 2.5$ Hz, 2H), 8.22 (s, 1H), 8.00 (d, $J = 7.0$ Hz, 1H), 7.92 (d, $J = 6.5$ Hz, 1H), 7.88–7.85 (m, 2H), 7.77–7.74 (m, 2H), 7.65 (d, $J = 3.5$ Hz, 2H), 7.22 (d, $J = 8.5$ Hz, 4H), 7.16–7.14 (m, 12H), 2.57 (t, 8H), 1.61–1.58 (m, 8H), 1.35–1.25 (m, 24H), 0.87–0.85 (m, 12H). FT-IR (cm⁻¹): 2216 (–CN), 1701 (C=O), 1282 (O=S=O). Mass (FAB, m/z): calcd for C₉₃H₈₂N₄O₃S₅: 1464.00 found: 1463 (M⁺). Anal. Calcd for C₉₃H₈₂N₄O₃S₅: C, 76.30; H, 5.65; N, 3.83. Found: C, 75.91; H, 5.64; N, 3.56%.



3. Electrochemical Properties of IND Derivatives

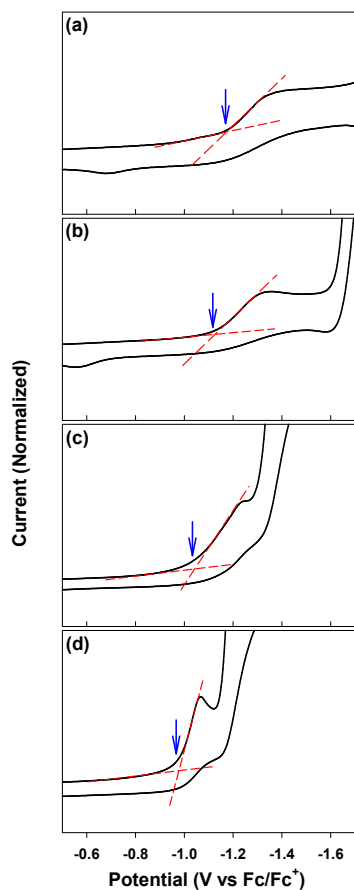


Fig. S1 Cyclic voltammograms of IND derivatives in the solution of CH₂Cl₂. (a) BTD, (b) BTDF, (c) IC, and (d) ICS.

Table S1. Summary of reduction potentials and LUMO levels for BTDF, BTDF, IC, and ICS units

	BTDF	BTDF	IC	ICS
E_{red} (V) ^a	-1.16	-1.11	-1.04	-0.98
E_{LUMO} (eV) ^b	-2.46	-2.67	-3.19	-3.50

^aFirst onset reduction potential vs Fc/Fc⁺. ^bDetermined using DFT calculations (B3LYP/6-31G*).

4. Thermal Properties of ITIC Derivatives

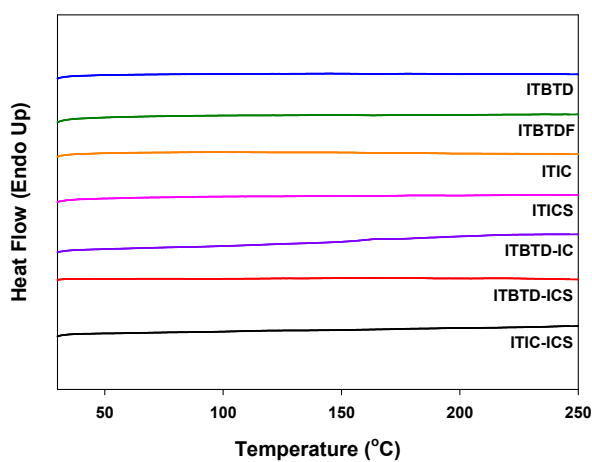


Fig. S2 DSC curves of symmetric and asymmetric ITIC derivatives measured at a heating rate of 10 °C min⁻¹ under N₂.

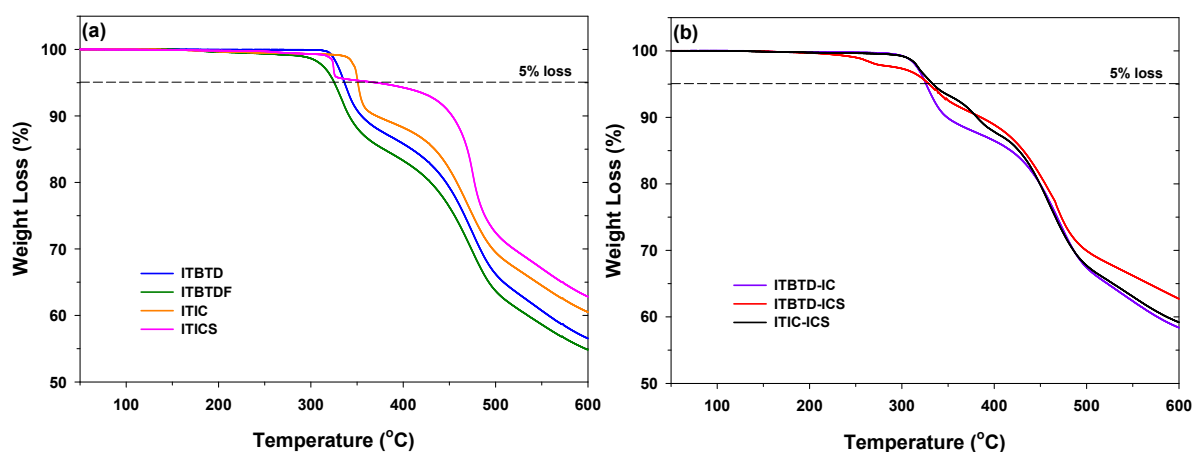


Fig. S3 TGA traces of (a) symmetric and (b) asymmetric ITIC derivatives measured at a heating rate of 10 °C min⁻¹ under N₂.

5. Optical Properties and Energy Levels of ITIC Derivatives in Film

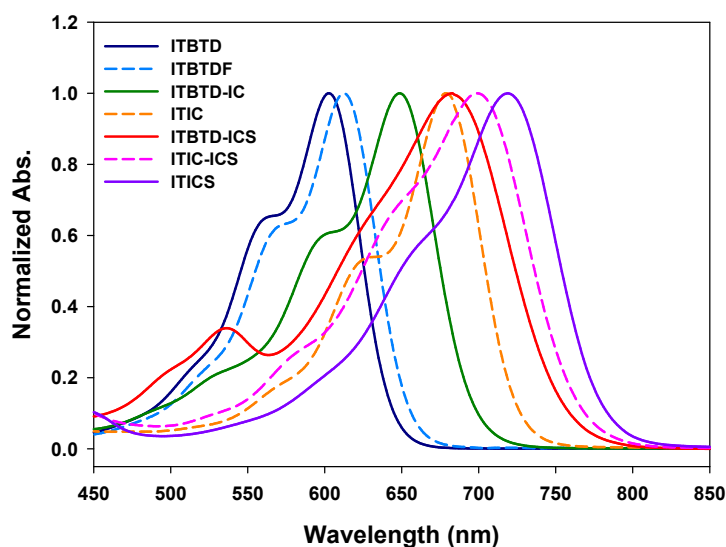


Fig. S4 UV/vis absorption spectra of symmetric and asymmetric ITIC derivatives in film.

Table S2. Summary of optical properties and energy levels of ITIC derivatives in film

Compound	$\lambda_{\text{max}}^{\text{a}}$ (nm)	E_{g}^{b} (nm)	$E_{\text{HOMO}}^{\text{c}}$ (eV)	$E_{\text{LUMO}}^{\text{d}}$ (eV)
ITBTD	594	1.92	-5.70	-3.78
ITBTDF	619	1.84	-5.78	-3.94
ITIC	707	1.60	-5.73	-4.14
ITICS	718	1.52	-5.82	-4.30
ITBTD-IC	648	1.72	-5.71	-3.99
ITBTD-ICS	670	1.62	-5.76	-4.13
ITIC-ICS	708	1.53	-5.75	-4.23

^aMeasured in film. ^bCalculated optical band gap using $E_{\text{g}}^{\text{opt}} = 1240/\lambda_{\text{onset}}^{\text{film}}$. ^cObtained from photoemission spectroscopy (AC-2). ^dDetermined using $E_{\text{HOMO}} = (E_{\text{LUMO}} - E_{\text{g}}^{\text{opt}})$ eV.

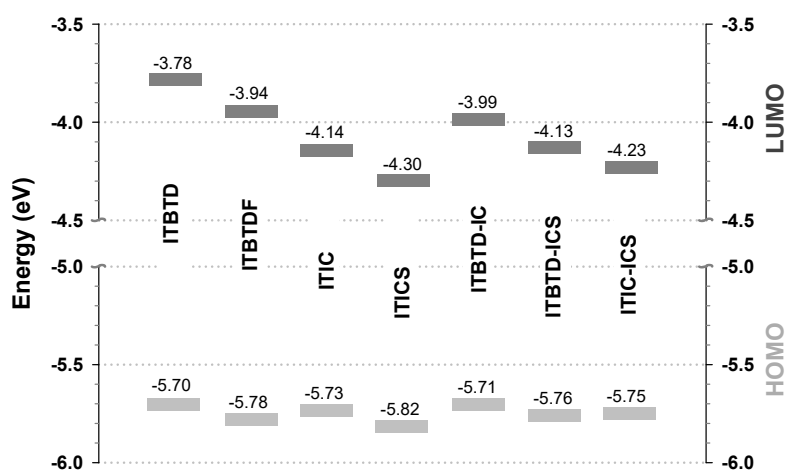


Fig. S5 HOMO and LUMO energy levels of ITIC derivatives calculated using photoemission spectroscopy (AC-2) and the equation of $E_{\text{HOMO}} = (E_{\text{LUMO}} - E_{\text{g}}^{\text{opt}})$ eV, respectively.

6. Orbital diagrams of ITIC Derivatives Calculated by DFT calculations

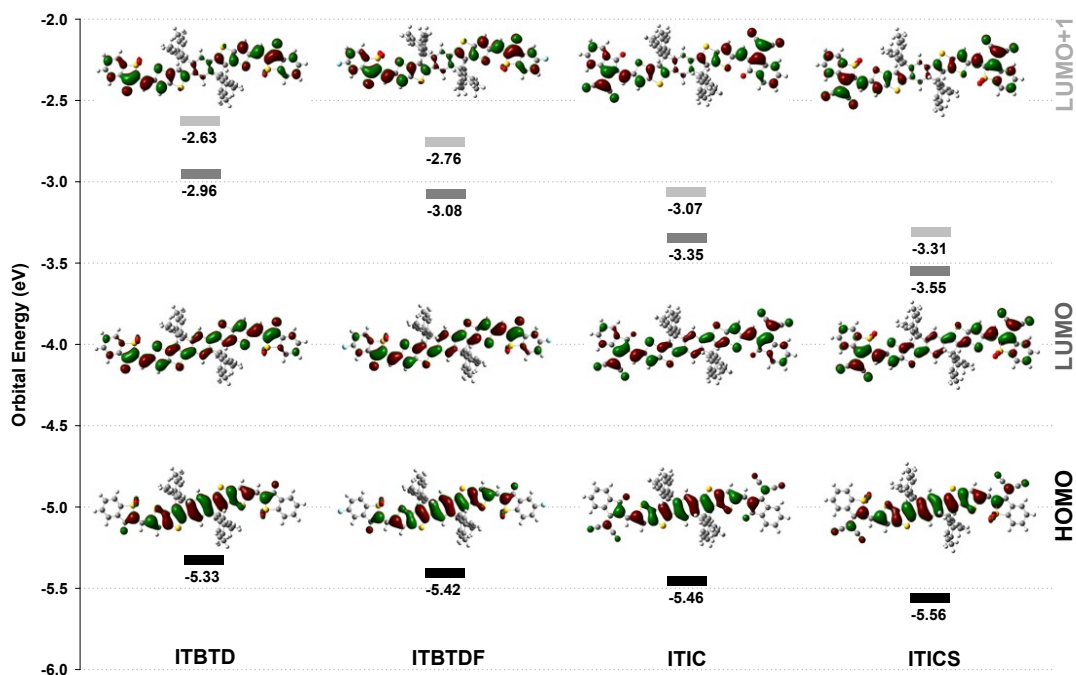


Fig. S6 Orbital diagrams of the HOMO, LUMO, and LUMO+1 of symmetric ITIC derivatives computed at the level of B3LYP/6-31G(d,p).

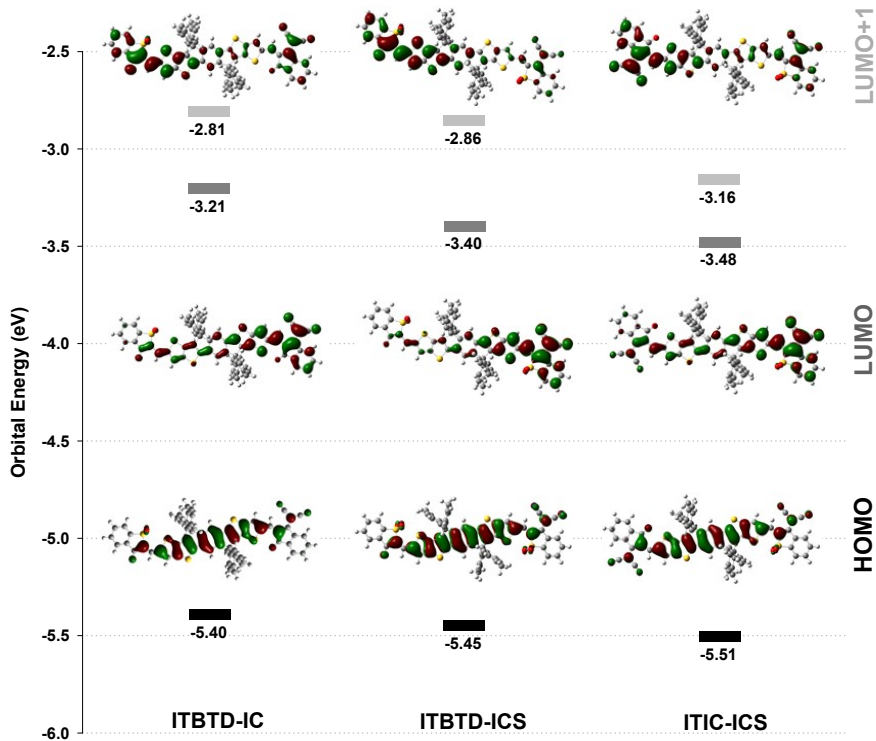


Fig. S7 Orbital diagrams of the HOMO, LUMO, and LUMO+1 of asymmetric ITIC derivatives computed at the level of B3LYP/6-31G(d,p).

7. PBDB-T:Acceptors-based Binary Solar Cells

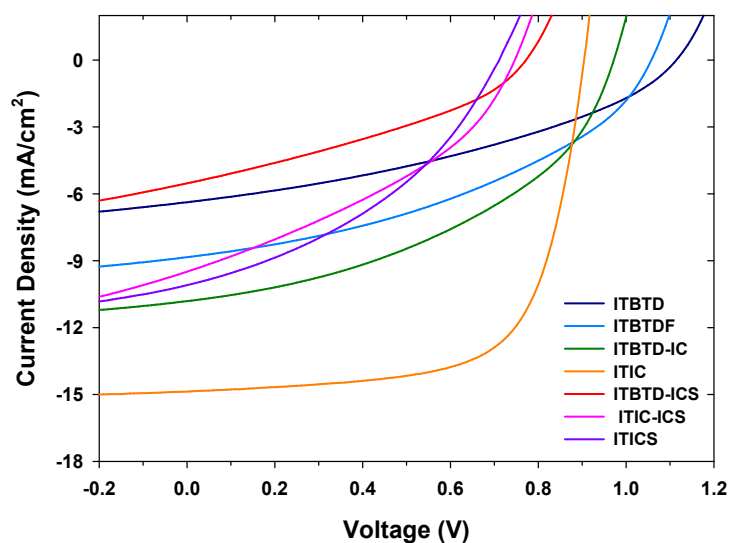


Fig. S8 J - V curves of the PBDB-T:acceptors-based binary solar cells.

Table S3. Energy loss of the PBDB-T:acceptors-based binary solar cells

Acceptor	E_{loss} (eV) ^a
ITBTD	0.70
ITBTDF	0.75
ITIC	0.70
ITICS	0.81
ITBTD-IC	0.75
ITBTD-ICS	0.85
ITIC-ICS	0.78

^aDetermined using $E_{\text{loss}} = (E_{\text{g}}^{\text{opt}} - eV_{\text{oc}})$, where $E_{\text{g}}^{\text{opt}}$ is the lowest energy bandgap of the donor and acceptor components

Table S4. Summary of hole and electron mobility of the SCLC devices of PBDB-T:ITIC derivatives blends

Active layer	Hole mobility (μ_h)	Electron mobility (μ_e)	μ_h / μ_e
	[$\text{cm}^2 \text{V}^{-1} \text{s}^{-1}$]	[$\text{cm}^2 \text{V}^{-1} \text{s}^{-1}$]	
PBDB-T:ITBTD	2.85×10^{-4}	4.99×10^{-5}	5.71
PBDB-T:ITBTDF	4.19×10^{-4}	8.70×10^{-5}	4.82
PBDB-T:ITIC	4.53×10^{-4}	4.28×10^{-4}	1.06
PBDB-T:ITICS	1.95×10^{-4}	2.13×10^{-5}	9.15
PBDB-T:ITBTD-IC	4.27×10^{-4}	9.49×10^{-5}	4.50
PBDB-T:ITBTD-ICS	8.48×10^{-5}	2.01×10^{-5}	4.22
PBDB-T:ITIC-ICS	1.29×10^{-4}	2.23×10^{-5}	5.78

8. DFT-Optimized Structures of ITIC, ITBTD and ITICS

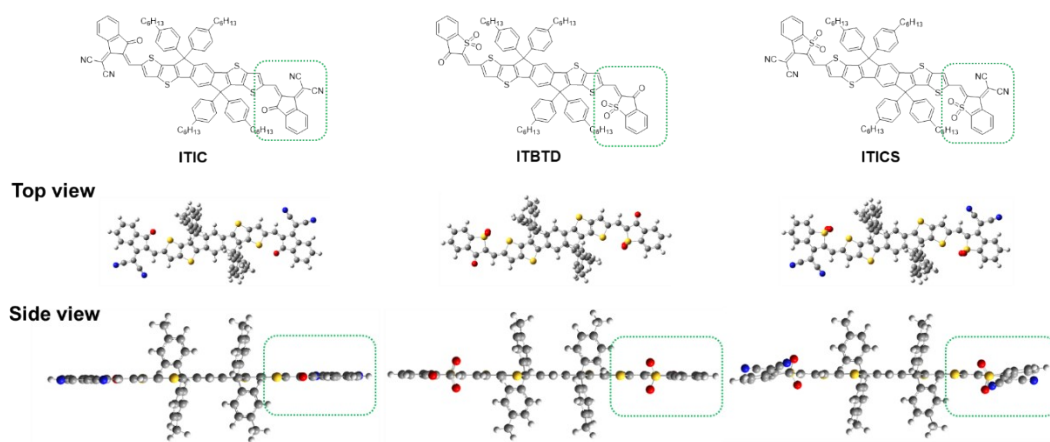


Fig. S9 Top and side views of the DFT-optimized structure of ITIC, ITBTD and ITICS.

9. PBDB-T:ITIC:A₂ Acceptor-based Ternary Solar Cells

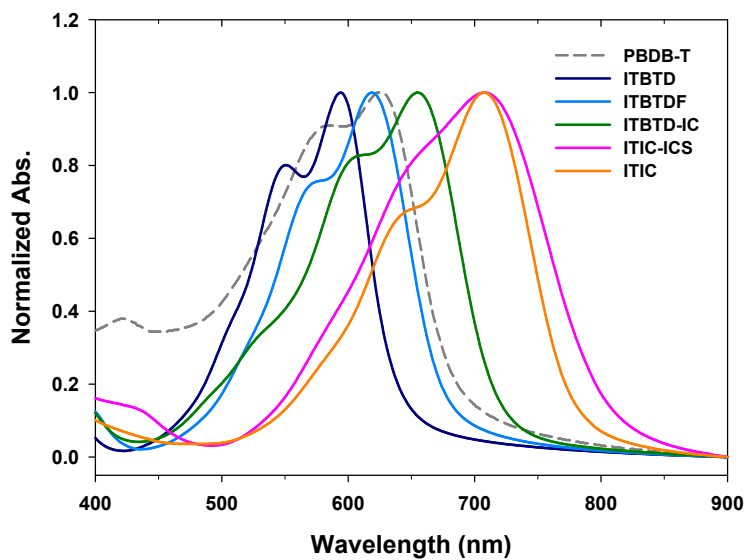


Fig. S10 UV/vis absorption spectra of PBDB-T donor polymer and acceptor molecules in film.

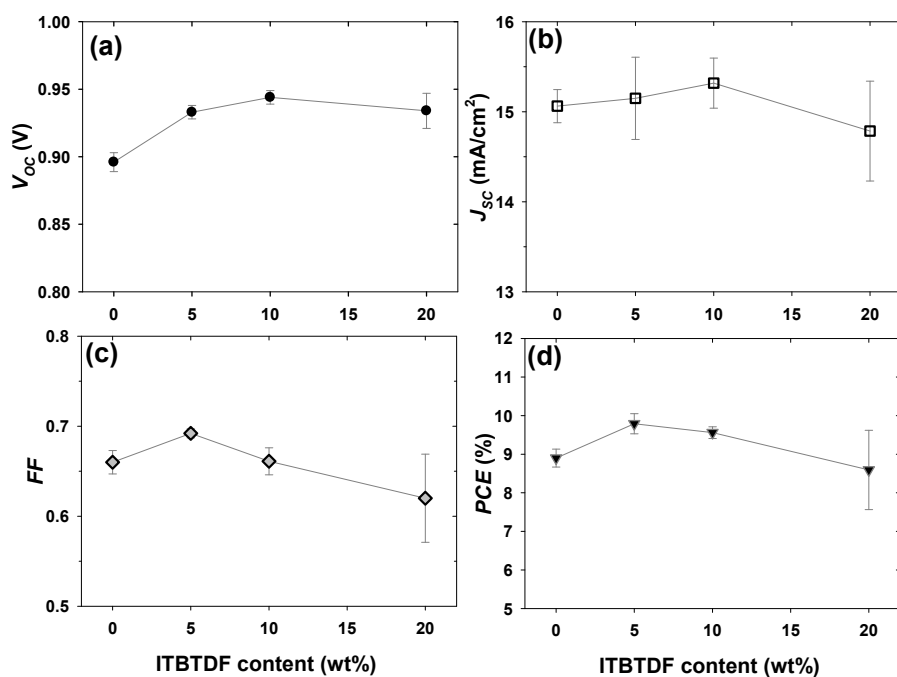


Fig. S11 The changes of (a) V_{OC} , (b) J_{SC} , (c) FF and (d) PCE as a function of ITBTDF (A_2 acceptor) content in PBDB-T:ITIC:ITBTDF-based ternary solar cells.

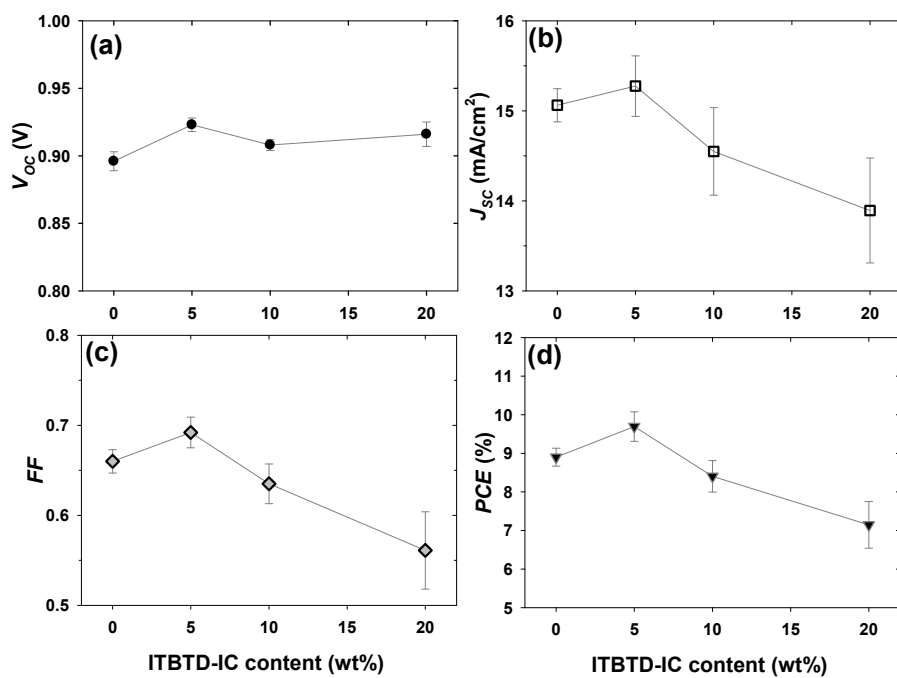


Fig. S12 The changes of (a) V_{OC} , (b) J_{SC} , (c) FF and (d) PCE as a function of ITBTD-IC (A_2 acceptor) content in PBDB-T:ITIC:ITBTD-IC-based ternary solar cells.

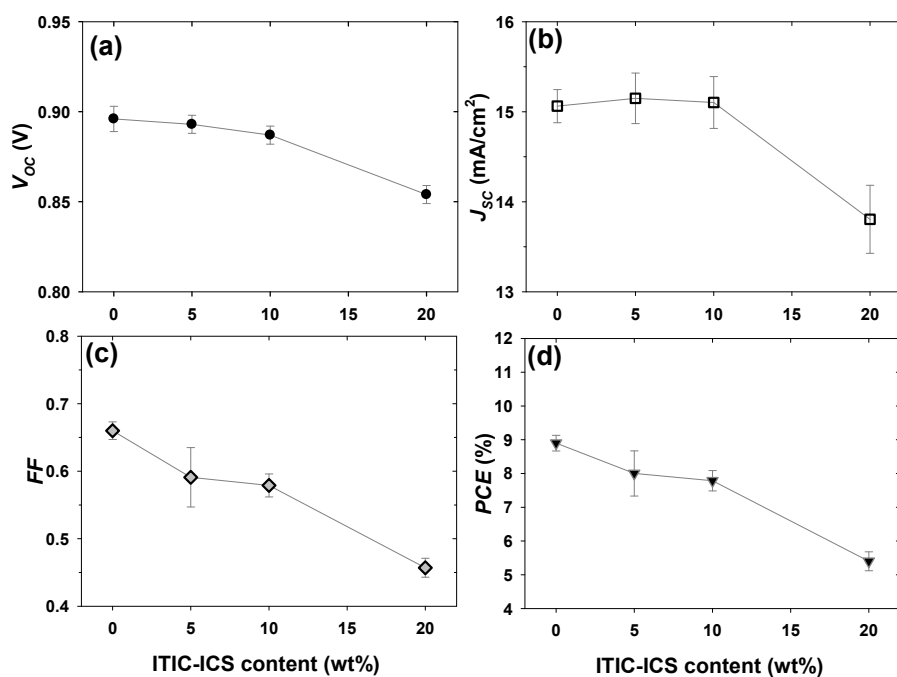


Fig. S13 The changes of (a) V_{OC} , (b) J_{SC} , (c) FF and (d) PCE as a function of ITIC-ICS (A_2 acceptor) content in PBDB-T:ITIC:ITIC-ICS-based ternary solar cells.

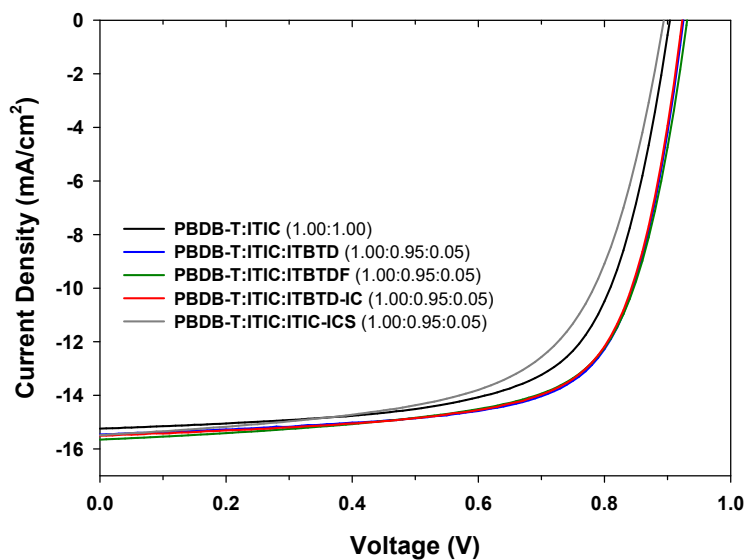


Fig. S14 J - V curves of the PBDB-T:ITIC: A_2 acceptor-based ternary solar cells.

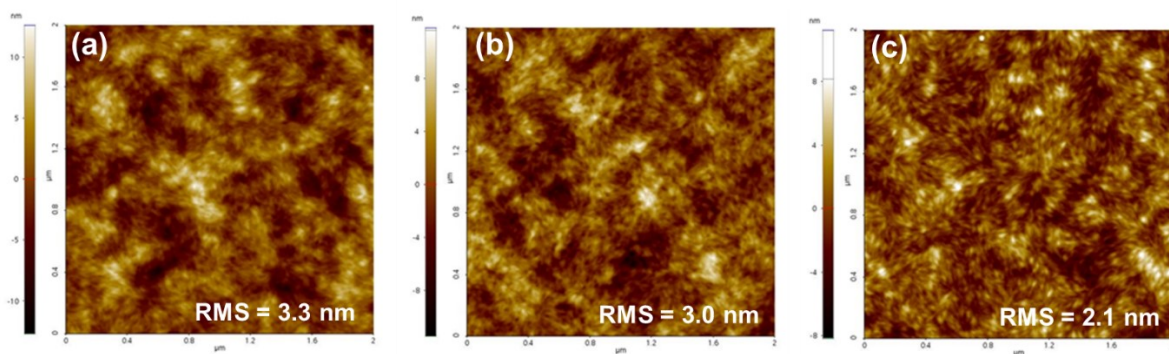


Fig. S15 AFM phase images and RMS values for (a) PBDB-T:ITIC, (b) PBDB-T:ITIC:ITBTD (1.00:0.95:0.05), and (c) PBDB-T:ITBTD blend films.

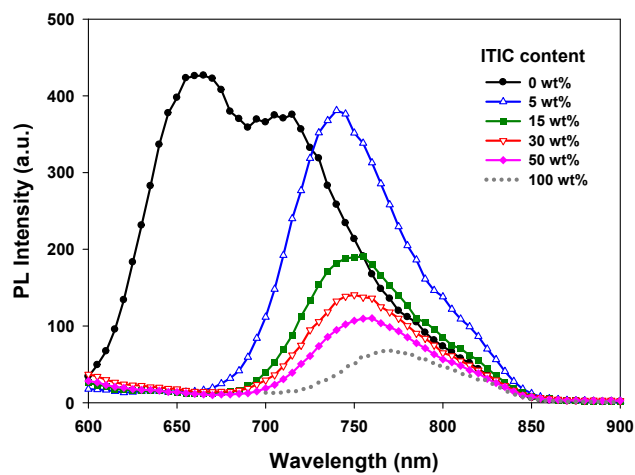


Fig. S16 Photoluminescence (PL) spectra of ITIC:ITBTD blend films with different ITIC content under 550 nm light excitation. The PL intensity of ITIC (100 wt% content) excited at 650 nm is normalized for comparison.

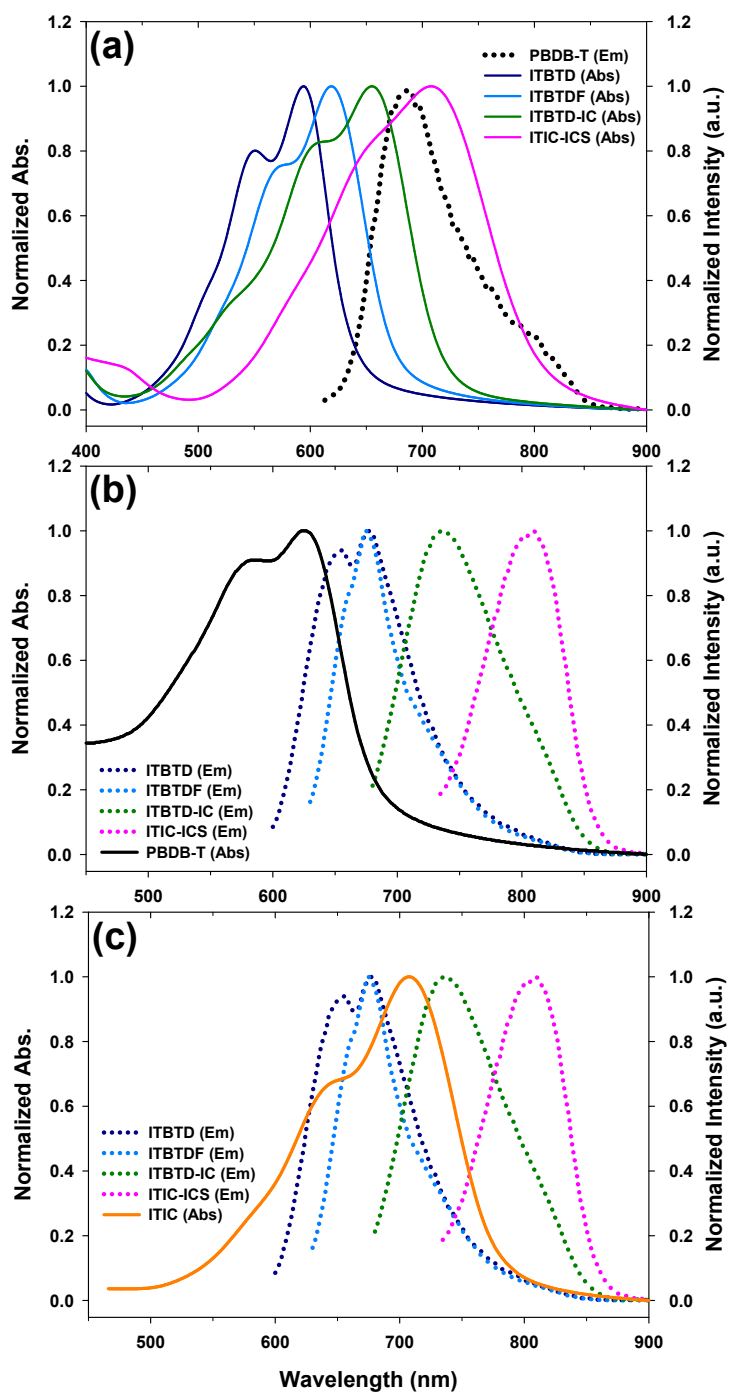


Fig. S17 (a) UV/vis absorption spectra of A_2 acceptor molecules and PL spectrum of PBDB-T donor polymer in film. (b) UV/vis absorption spectrum of PBDB-T donor polymer and PL spectra of A_2 acceptor molecules in film. (c) UV/vis absorption spectrum of ITIC and PL spectra of A_2 acceptor molecules in film.

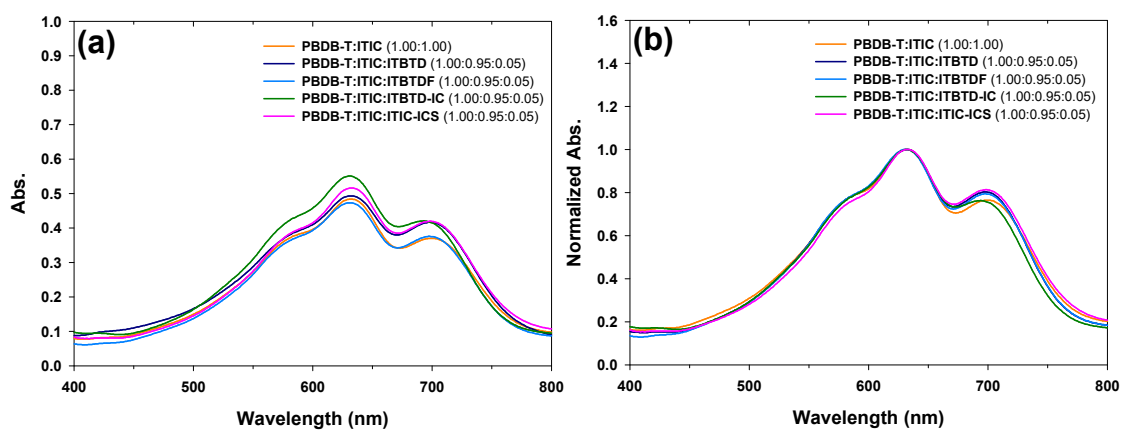


Fig. S18 (a) UV/vis absorption spectra of PBDB-T:ITIC and PBDB-T:ITIC:A₂ acceptor in film. (b) Same graphs as for (a) but normalized to absorption at 632 nm.